Science Advances

AAAS

advances.sciencemag.org/cgi/content/full/2/3/e1501602/DC1

Supplementary Materials for

Universal dependence of hydrogen oxidation and evolution reaction activity of platinum-group metals on pH and hydrogen binding energy

Jie Zheng, Wenchao Sheng, Zhongbin Zhuang, Bingjun Xu, Yushan Yan

Published 18 March 2016, *Sci. Adv.* **2**, e1501602 (2016)
DOI: 10.1126/sciadv.1501602

The PDF file includes:

Supplementary Materials

1. Derivation of relationship between i_0 and E_{peak}

Arrhenius equation

$$i_0 = K\exp(-\frac{E_a}{RT}) \qquad \text{(S1.1)}$$

where i_0 is the exchange current density, K is the pre-exponential parameter, E_a is the activation energy, R is the gas constant, and T is the temperature in Kelvin.

Brønsted-Evans-Polanyi principle states that the activation energy is proportional to the reaction enthalpy for reactions in the same family, more specifically:

$$E_a = E_0 + \beta\Delta H \qquad \text{(S1.2)}$$

where E_0 is the activation energy of a reaction in the same family, ΔH is the enthalpy of reaction, and β is a proportionality coefficient that characterizes the position of transition state along the reaction coordinate ($0 \le \beta \le 1$).

For HOR/HER ($H_2 \leftrightarrow 2H^+ + 2e$), it consists of either a Tafel step ($H_2 + 2* \leftrightarrow 2H_{ad}$) or a Heyrovsky step ($H_2 + * \leftrightarrow H_{ad} + H^+ + e$) followed by a Volmer step ($H_{ad} \leftrightarrow H^+ + e + *$). If the Volmer step is the rate-determining step, the activation energy of HOR/HER is approximately the activation energy of the Volmer step

$$E_a = E_{a,Volmer} = E_0 + \beta\Delta H_{H,desorption} \qquad \text{(S1.3)}$$

It has been derived earlier(*25*) that

$$-\Delta H_{H,desorption} = \Delta H_{H,ads} = -FE_{peak} - \frac{1}{2}TS^0_{H_2} \qquad \text{(S1.4)}$$

where $\Delta H_{H,desorption}$ is the enthalpy of H desorption, $\Delta H_{H,ads}$ is the enthalpy of H adsorption, E_{peak} is the H_{upd} desorption peak potential, $S^0_{H_2}$ is the standard entropy of H_2.

Hence, $E_a = E_0 + \beta(FE_{peak} + \frac{1}{2}TS^0_{H_2})$ (S1.5)

Substituting Eq. S1.5 into Eq. S1.1 yields

$$i_0 = K\exp(-\frac{E_0 + \beta(FE_{peak} + \frac{1}{2}TS^0_{H_2})}{RT}) = K\exp(-\frac{E_0 + \frac{1}{2}\beta TS^0_{H_2}}{RT})\exp(-\frac{\beta FE_{peak}}{RT})$$

Let $A = K\exp(-\frac{E_0 + \frac{1}{2}\beta TS^0_{H_2}}{RT})$

$$i_0 = A\exp(-\frac{\beta F E_{peak}}{RT}) \qquad \text{(S1.6)}$$

If $E_{a,1}$ and $E_{a,2}$ are the activation energies of HOR/HER at pH1 and pH2, respectively, while $E_{peak,1}$ and $E_{peak,2}$ are the H_{upd} desorption peak potentials at pH1 and pH2, respectively, then according to Eq. S1.5

$$E_{a,1} - E_{a,2} = \beta F(E_{peak,1} - E_{peak.2}) \qquad \text{(S1.7)}$$

2. Cyclic voltammograms of Pt/C, Ir/C, Pd/C, and Rh/C at different pH values

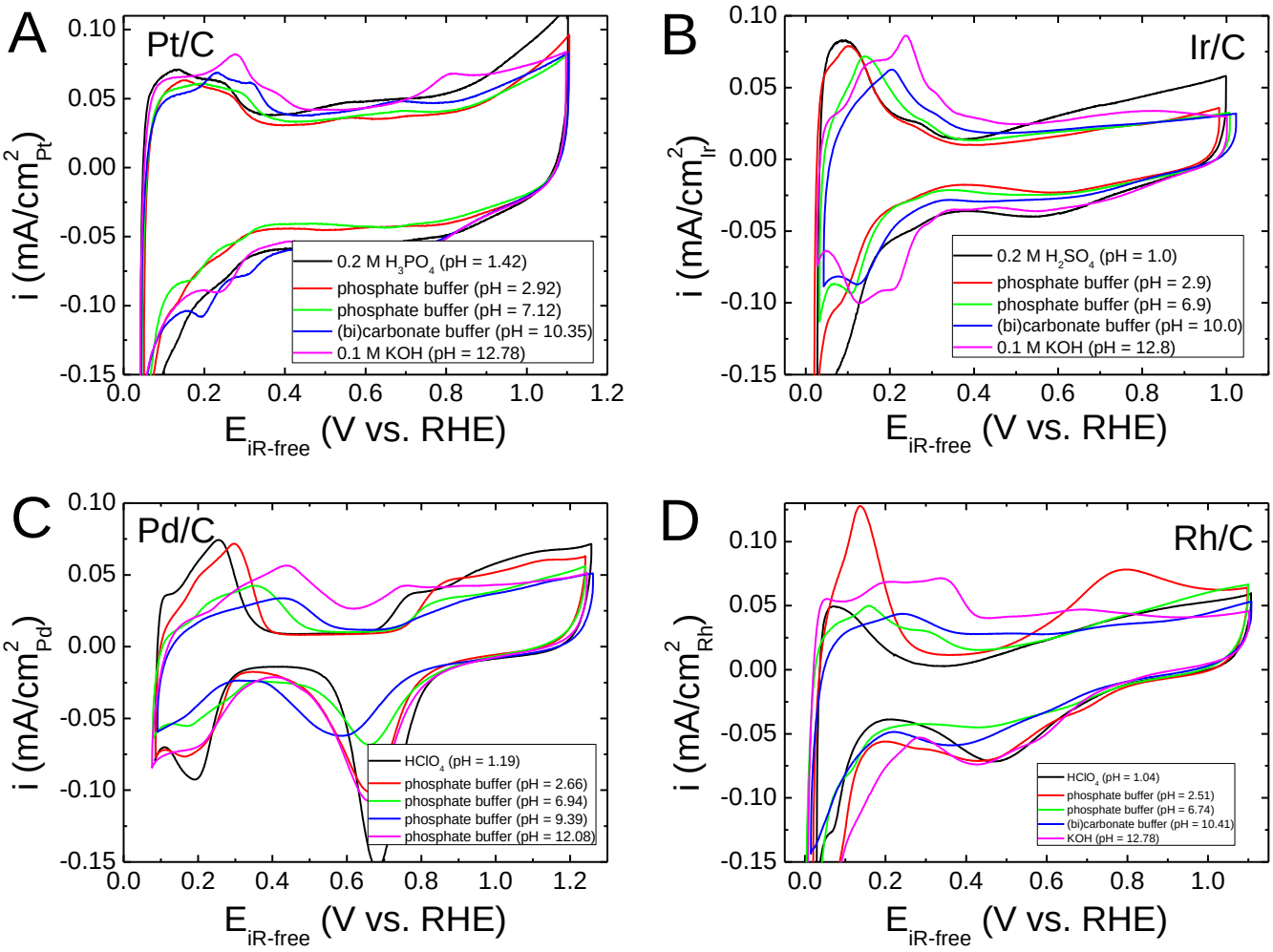

Fig. S1. CVs of Pt/C, Ir/C, Pd/C, and Rh/C at different pH values. Cyclic voltammograms (CVs) of (**A**) Pt/C, (**B**) Ir/C, (**C**) Pd/C and (**D**) Rh/C at different pHs (currents were normalized to $ECSA_{CV}$ measured in 0.1 M KOH).

3. CVs and HOR/HER polarization curves at different pH values

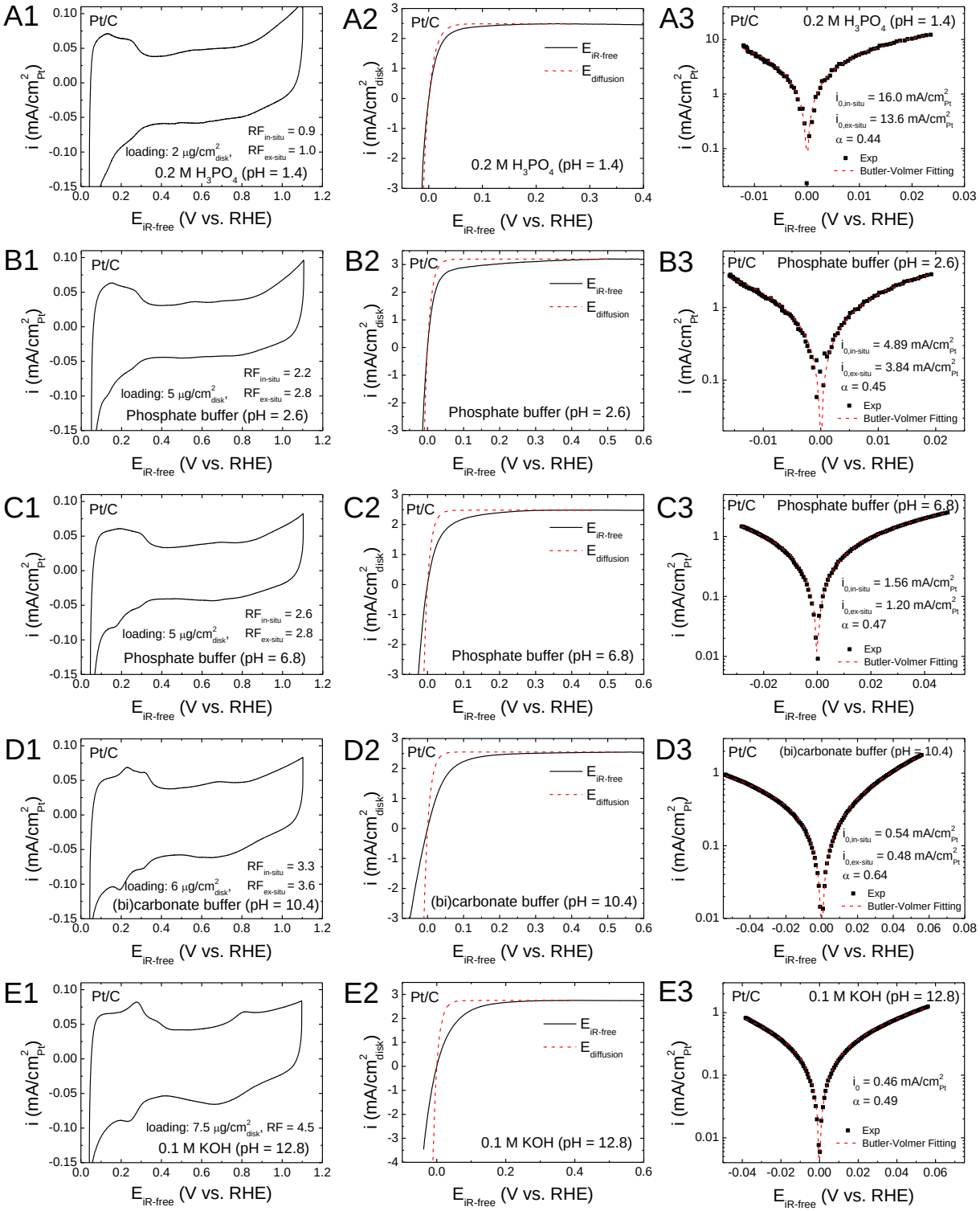

Fig. S2. CVs and HOR/HER polarization curves at different pH values on Pt/C. CVs (**A1-E1**), HOR/HER polarization curves (**A2-E2**), and kinetic current densities with fittings based on the Butler-Volmer equation with $\alpha_a + \alpha_c = 1$ (**A3-E3**) on Pt/C in electrolytes at different pH values. CVs were measured in Ar at a scanning rate of 50 mV/s. HOR/HER polarization curves were collected in H_2-saturated electrolytes at a scanning rate of 1 mV/s and a rotating speed of 1600 rpm.

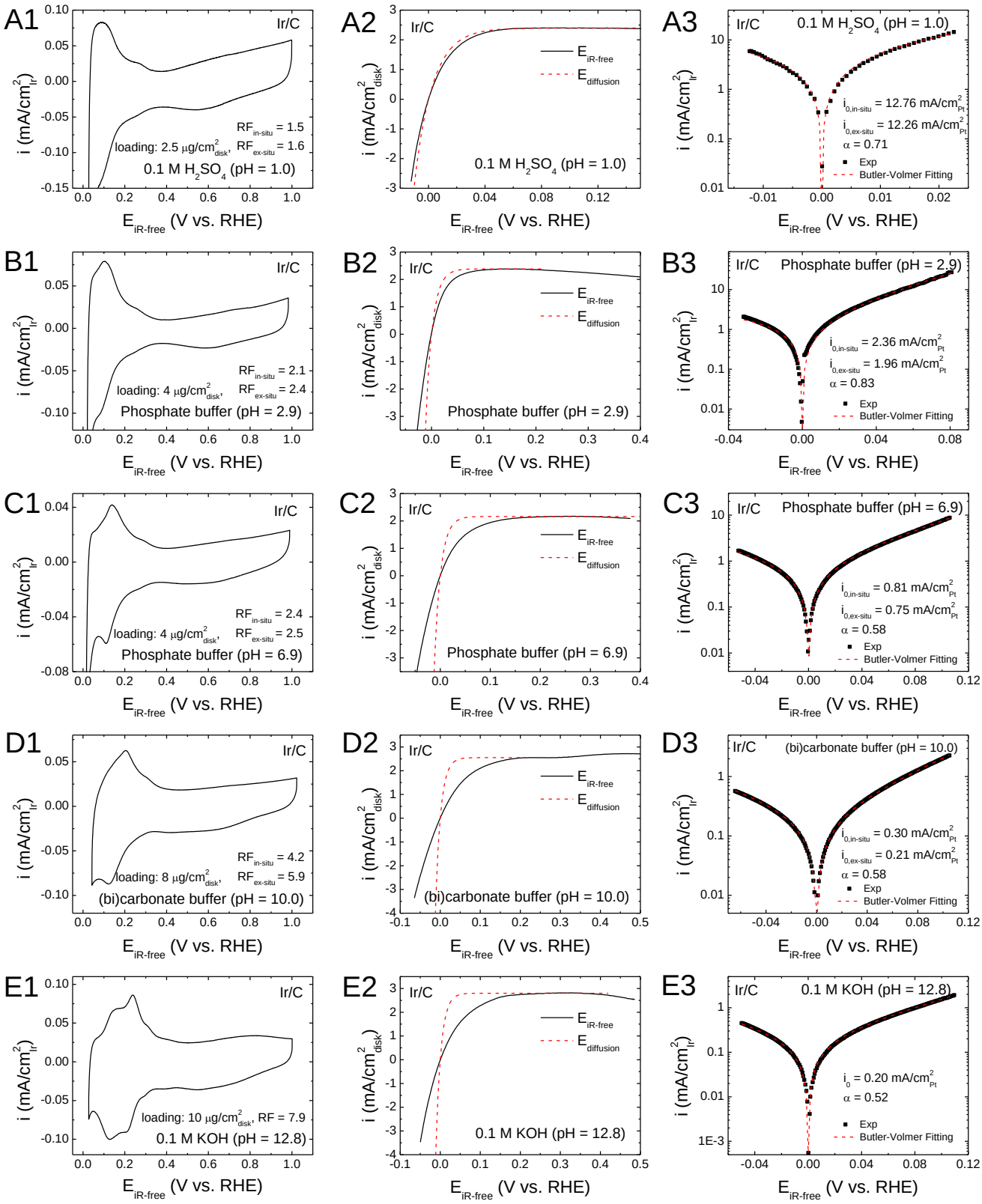

Fig. S3. CVs and HOR/HER polarization curves at different pH values on Ir/C. CVs (**A1-E1**), HOR/HER polarization curves (**A2-E2**), kinetic current density with their fitting into the Butler-Volmer equation with $\alpha_a + \alpha_c = 1$ (**A3-E3**) on Ir/C in electrolytes with different pH. CVs were measured in Ar at a scanning rate of 50 mV/s, HOR/HER polarization curves were collected in H_2-saturated electrolytes at a scanning rate of 1 mV/s and rotating speed of 1600 rpm.

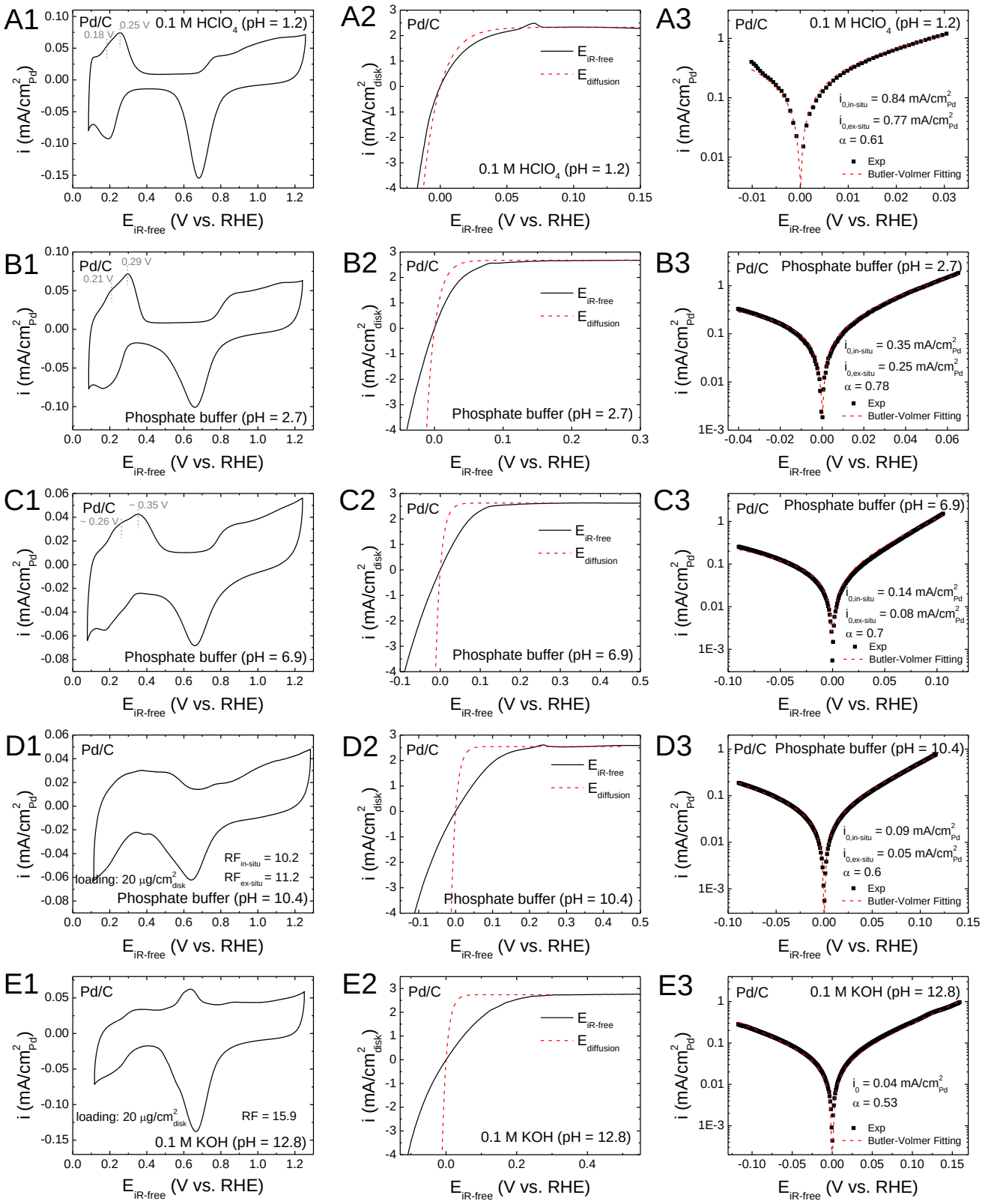

Fig. S4. CVs and HOR/HER polarization curves at different pH values on Pd/C.CVs (**A1-E1**), HOR/HER polarization curves (**A2-E2**), kinetic current density with their fitting into the Butler-Volmer equation with $\alpha_a + \alpha_c = 1$ (**A3-E3**) on Pd/C in electrolytes with different pH. CVs were measured in Ar at a scanning rate of 50 mV/s, HOR/HER polarization curves were collected in H_2-saturated electrolytes at a scanning rate of 1 mV/s and rotating speed of 1600 rpm.

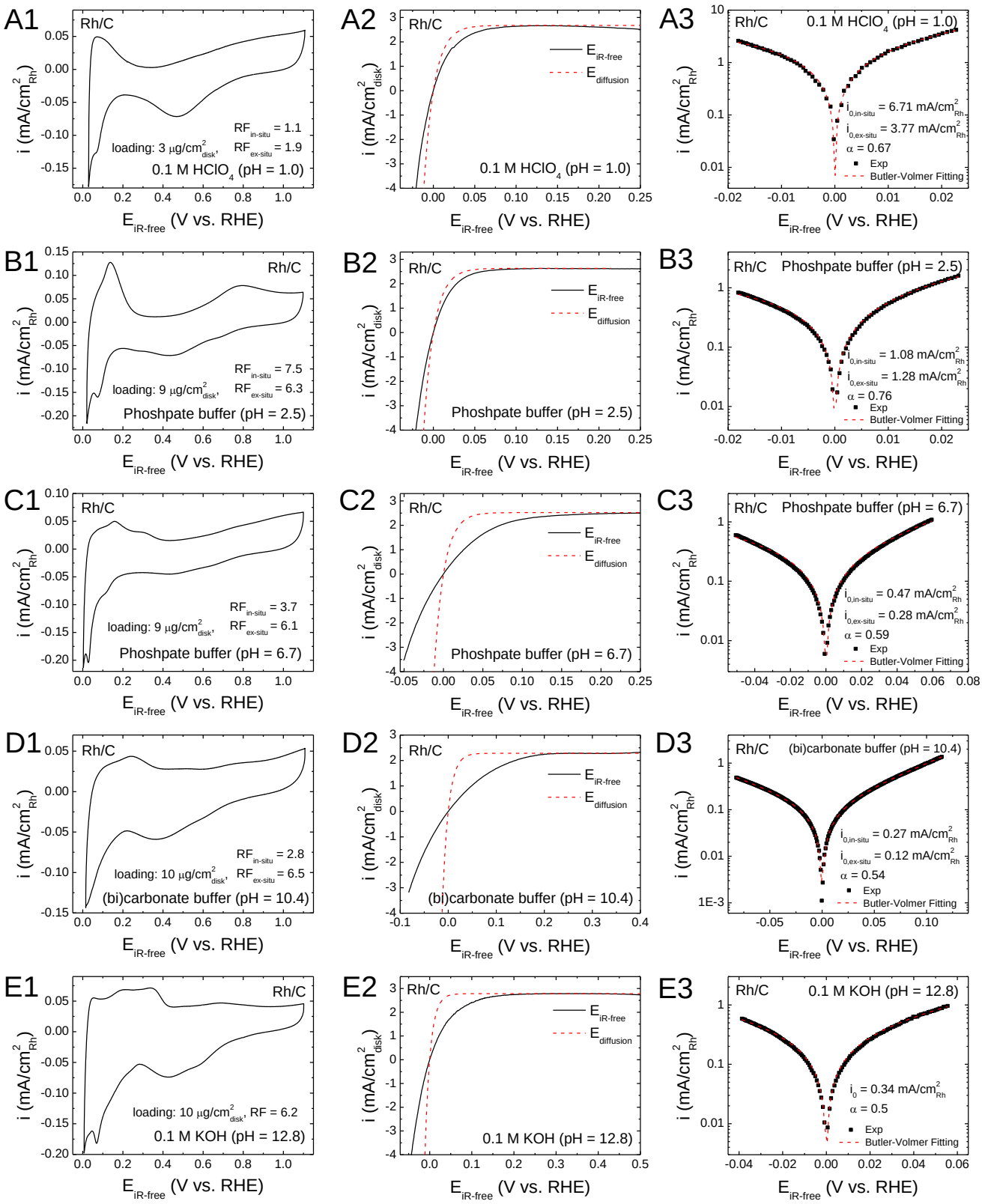

Fig. S5. CVs and HOR/HER polarization curves at different pH values on Rh/C. CVs (**A1-E1**), HOR/HER polarization curves (**A2-E2**), kinetic current density with their fitting into the Butler-Volmer equation with $\alpha_a + \alpha_c = 1$ (**A3-E3**) on Rh/C in electrolytes with different pH. CVs were measured in Ar at a scanning rate of 50 mV/s, HOR/HER polarization curves were collected in H_2-saturated electrolytes at a scanning rate of 1 mV/s and rotating speed of 1600 rpm.

4. Cyclic voltammograms (CVs)

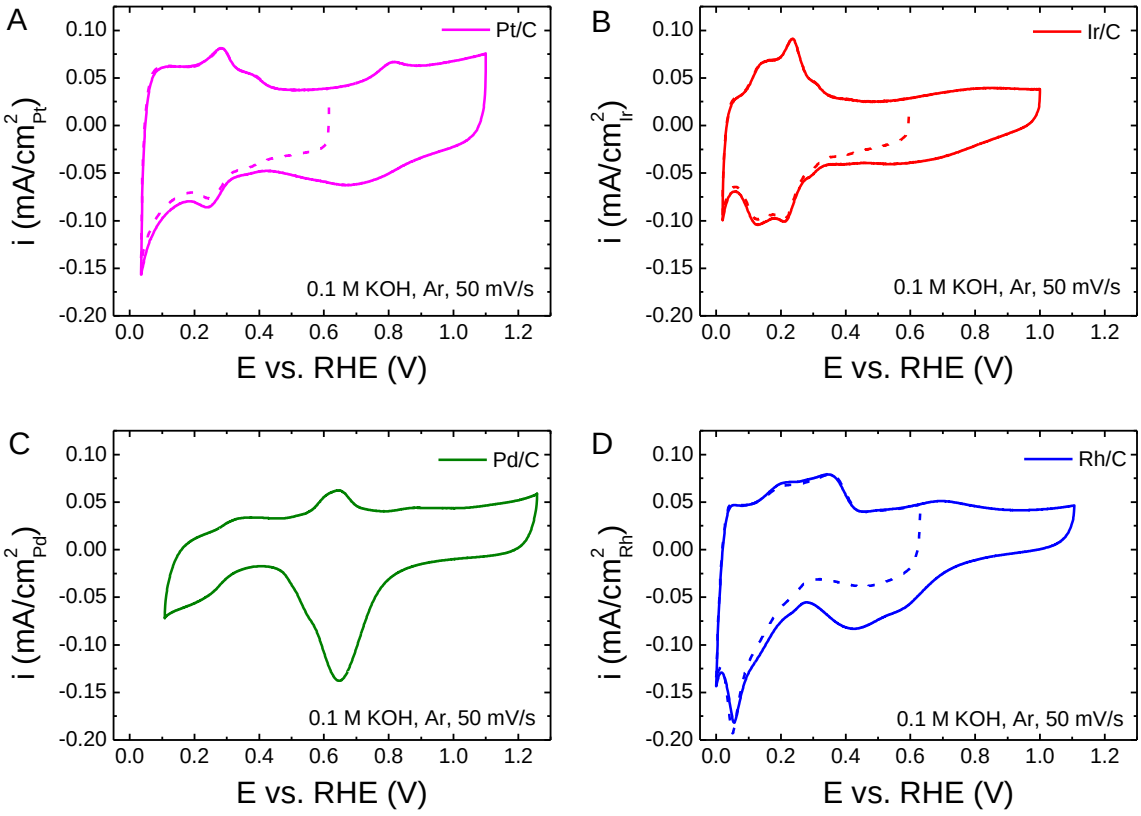

Fig. S6. CVs of Pt/C, Ir/C, Pd/C, and Rh/C in 0.1 M KOH. Cyclic voltammograms of (**A**) Pt/C, (**B**) Ir/C, (**C**) Pd/C and (**D**) Rh/C measured in Ar-saturated 0.1 M KOH with a scanning rate of 50 mV/s. The dash line represents CV scans in a small potential range to avoid the contribution of oxide reduction current to the H_{upd} adsorption current.

The electrochemical surface areas of Pt/C, Ir/C and Rh/C in this work were determined from the H_{upd} adsorption and desorption peaks while that of Pd/C was determined from PdO reduction peak, as described in the experimental section in manuscript and listed in Table S1 as $ECSA_{CV}$. The surface areas can also be determined from CO-stripping peak corresponding to a charge density of 420 $\mu C/cm^2$,(*46*) which were listed in Table S1 as $ECSA_{CO\text{-}stripping}$.

$ECSA_{CV}$ and $ECSA_{CO\text{-}stripping}$ of Pt/C, Ir/C, Pd/C and Rh/C (except $ECSA_{CO\text{-}stripping}$ of Rh/C) are smaller than their corresponding volume/surface averaged surface area ($S_{v/a}^{TEM}$), probably due to the partial covering of the particles by the carbon support. The $ECSA_{CO\text{-}stripping}$ is larger than $ECSA_{CV}$ for all four supported metals (Table S1). Similar results were obtained by Durst et al., and they suggested to normalize the HOR/HER kinetic currents by surface area determined from CO-stripping.(*24*) However, since we are studying the trends of activities vs pH or HBE, normalizing the activities by $ECSA_{CV}$ will not alter our conclusion as long as we follow the same protocol for all experiments. In addition, the difference between $ECSA_{CO\text{-}stripping}$ and $ECSA_{CV}$ is less than a factor of 2, which is not significant compared with the two-orders of magnitude difference of HOR/HER activity in acid and base.

5. Correlation of exchange current densities with E_{peak}

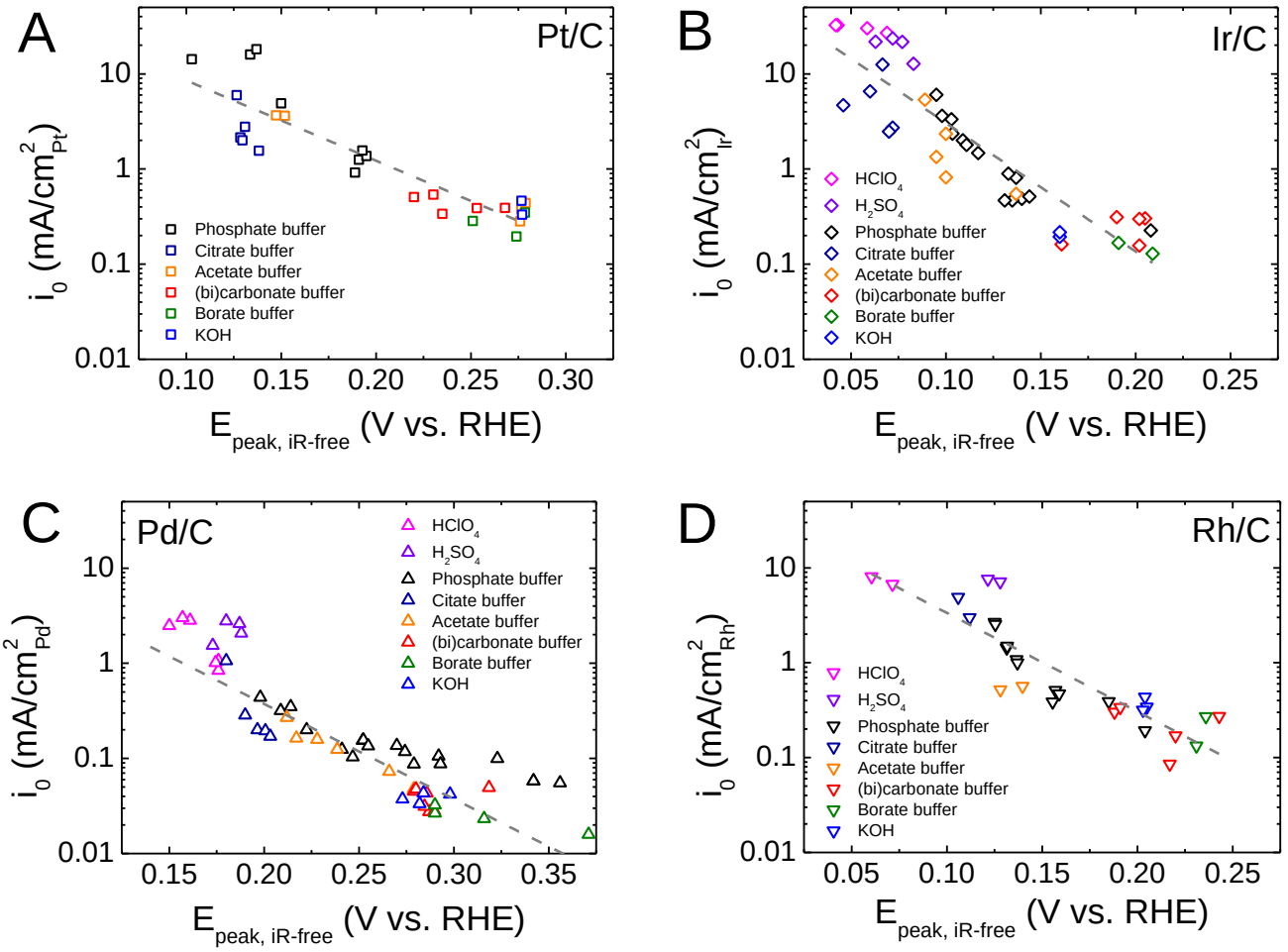

Fig. S7. Correlation of exchange current densities with E_{peak}. Exchange current densities of HOR/HER on (**A**) Pt/C, (**B**) Ir/C, (**C**) Pd/C and (**D**) Rh/C as a function of underpotential deposited hydrogen (H_{upd}) desorption peak potential (E_{peak}) from CVs. Gray dash lines in the four figures are linear fittings of the data.

6. Arrhenius Plot

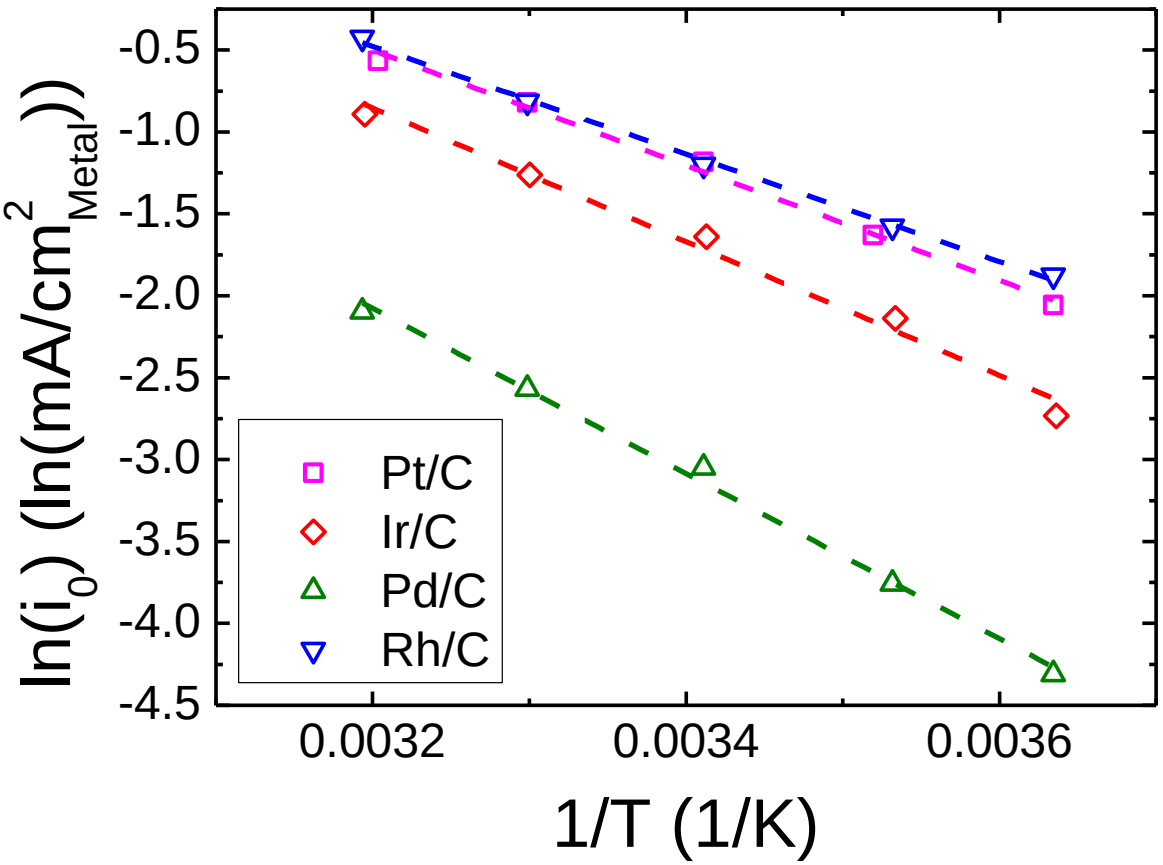

Fig. S8. Arrhenius plots of HOR/HER activities. Arrhenius plot of HOR/HER activities on Pt/C (square), Ir/C (diamond), Pd/C (up-triangle) and Rh/C (down-triangle) in 0.1 M KOH.

7. CO stripping in electrolytes with different pH values

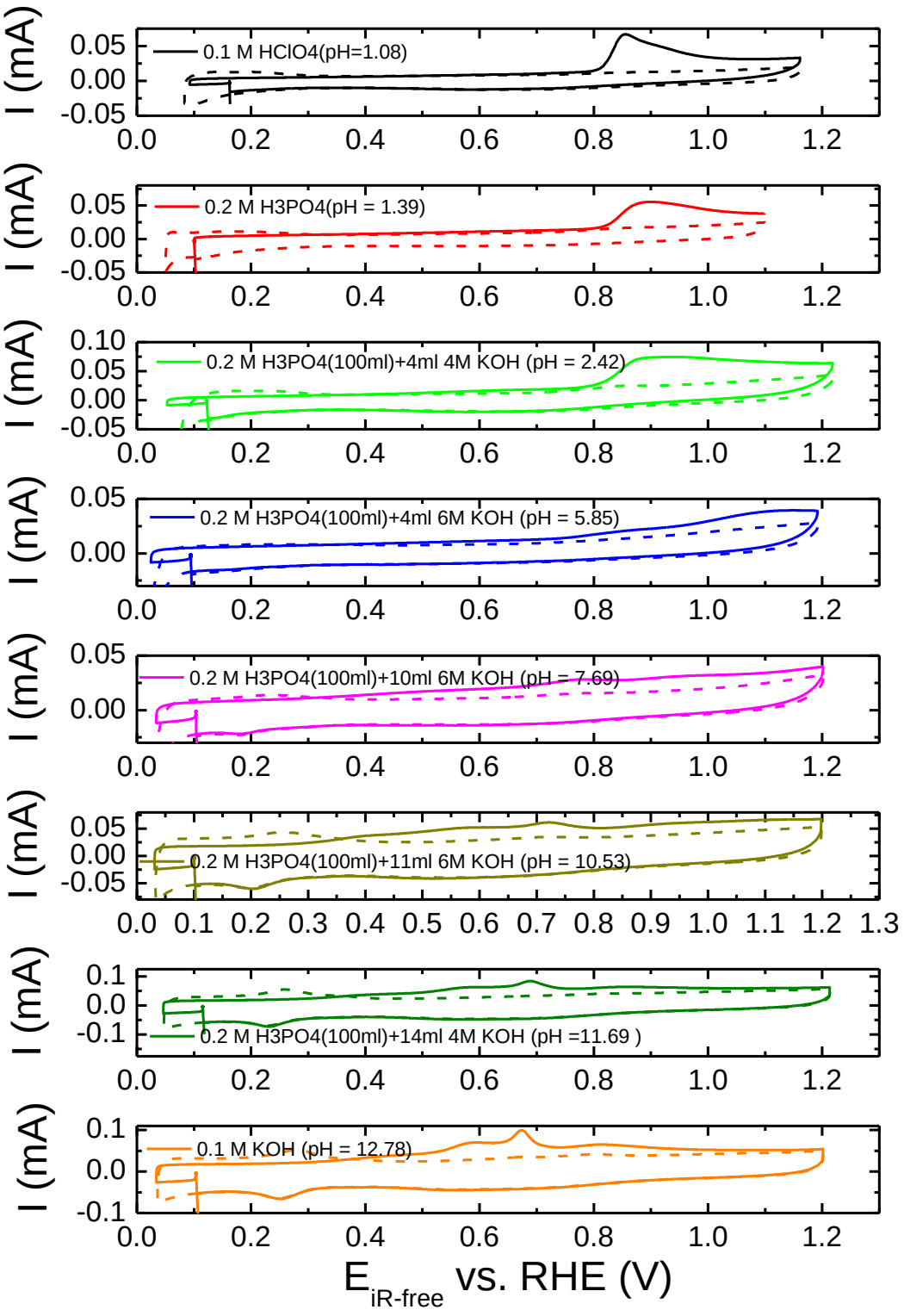

Fig. S9. CO stripping profiles on Pt/C at different pH values.

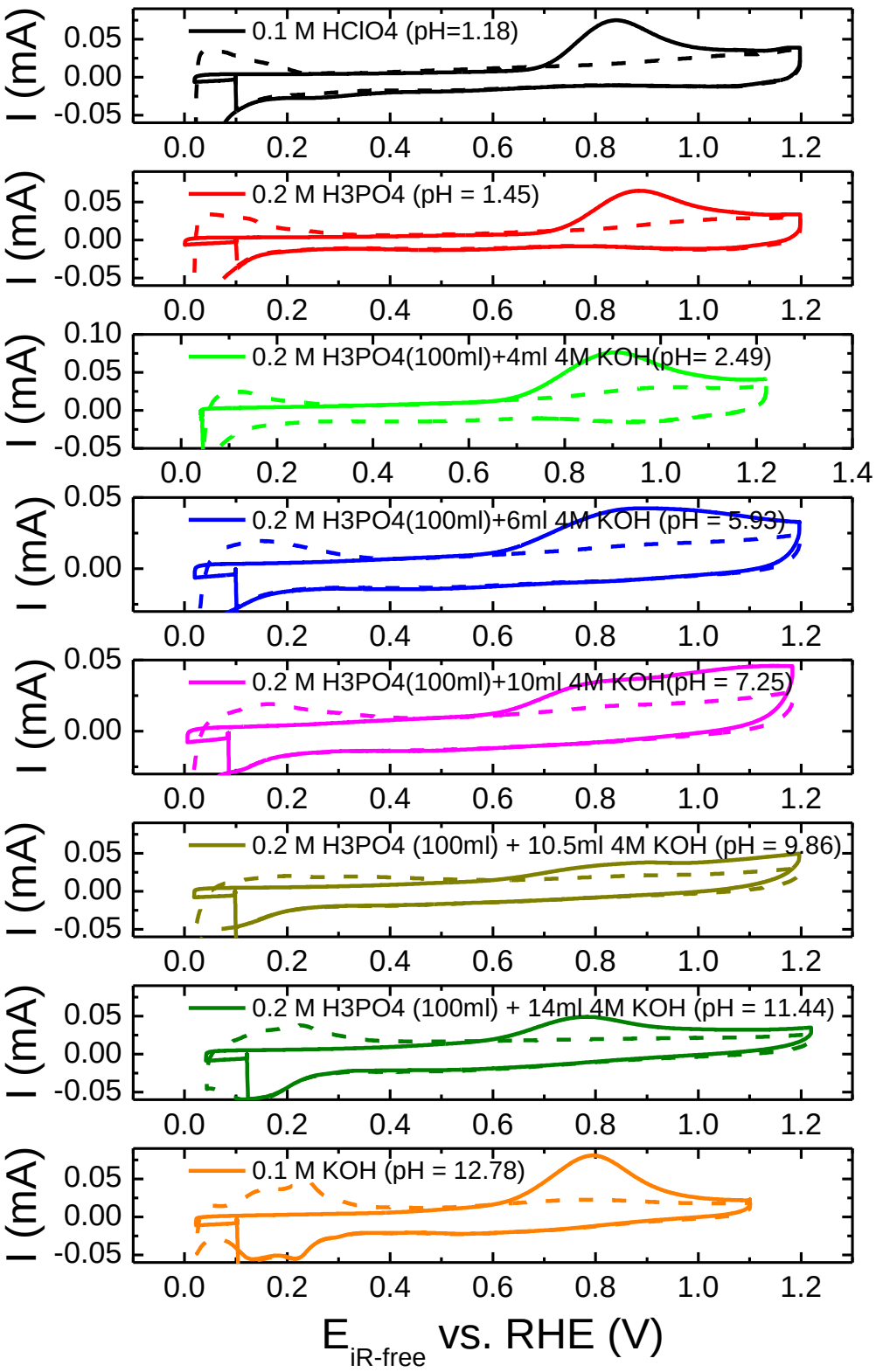

Fig. S10. CO stripping profiles on Ir/C at different pH values.

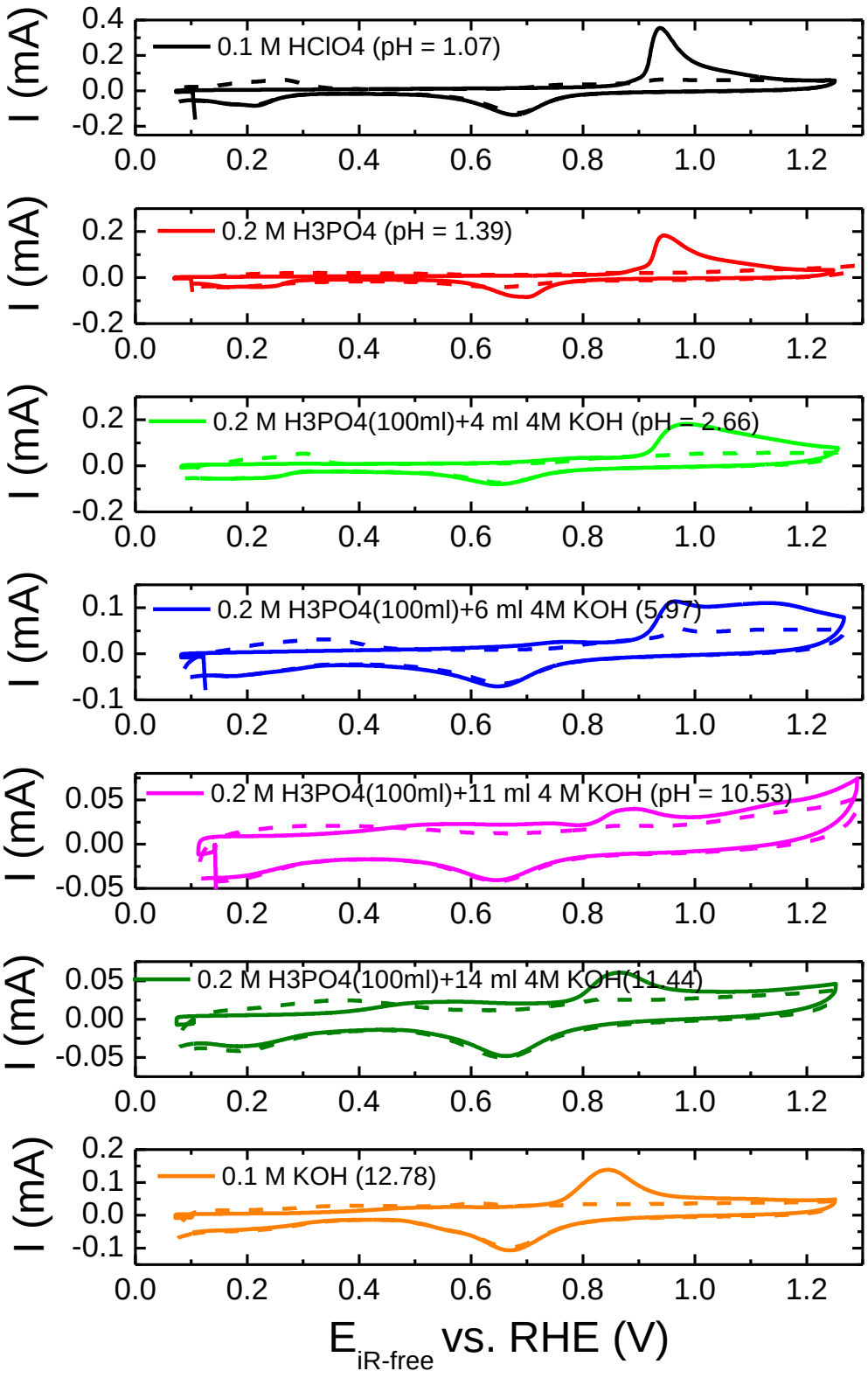

Fig. S11. CO stripping profiles on Pd/C at different pH values.

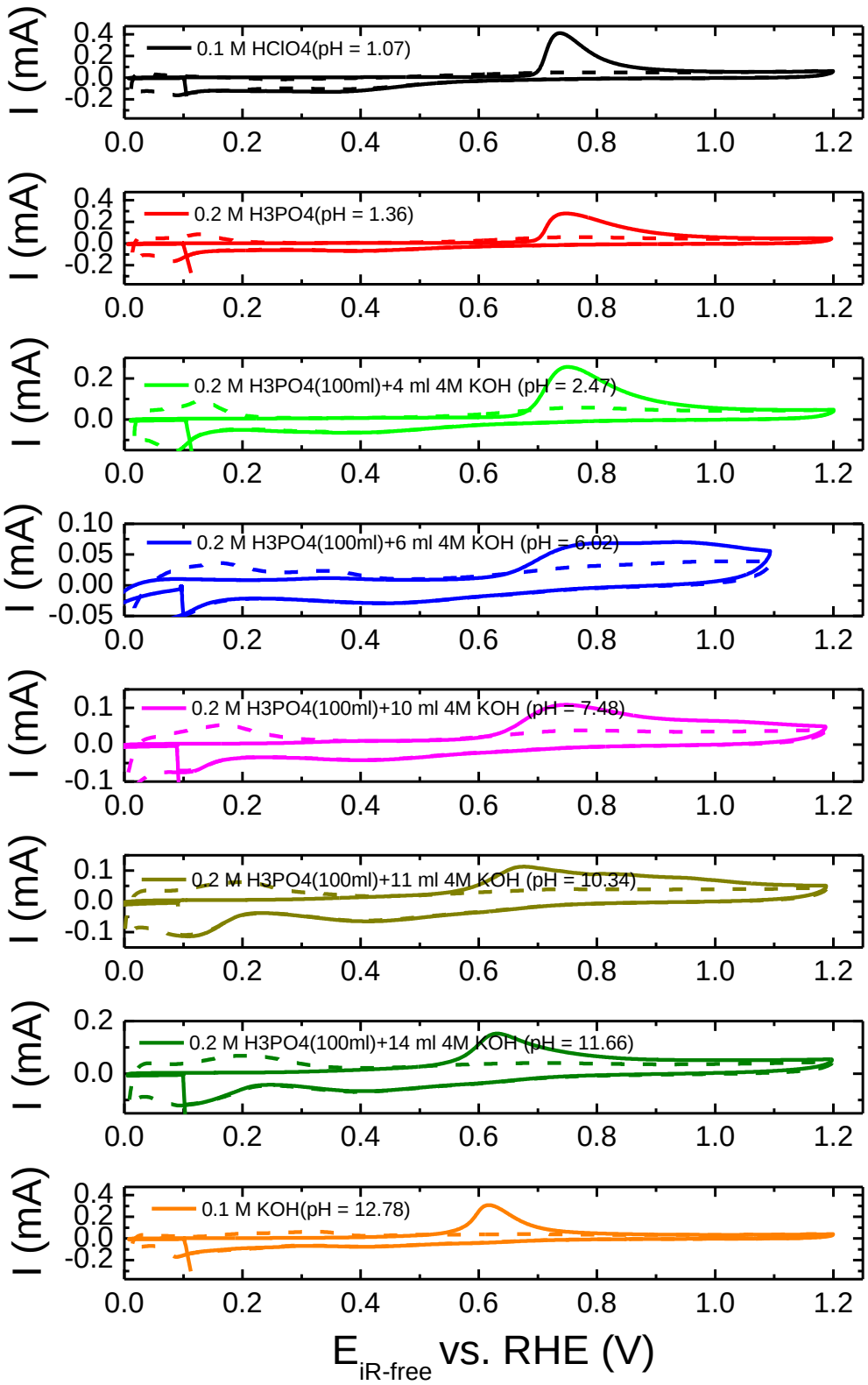

Fig. S12. CO stripping profiles on Rh/C at different pH values.

8. Effect of anions on HOR/HER activities

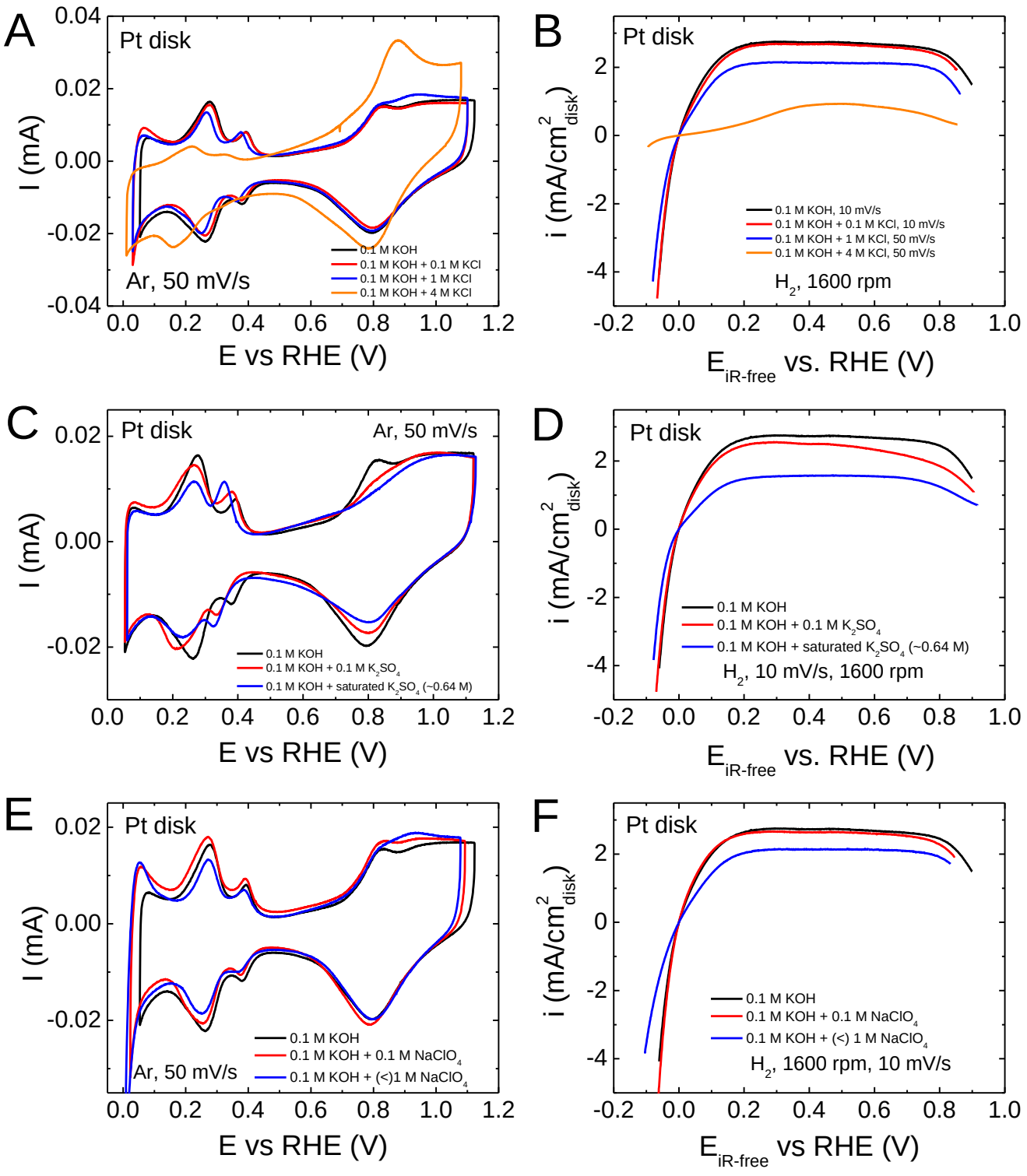

Fig. S13. Effect of anions on HOR/HER activities. CVs and the HOR/HER polarization curves on a Pt disk in 0.1 M KOH with additional salts of (**A, B**) KCl, (**C, D**) K_2SO_4, and (**E, F**) $NaClO_4$.

9. TEM images of supported metal electrocatalysts

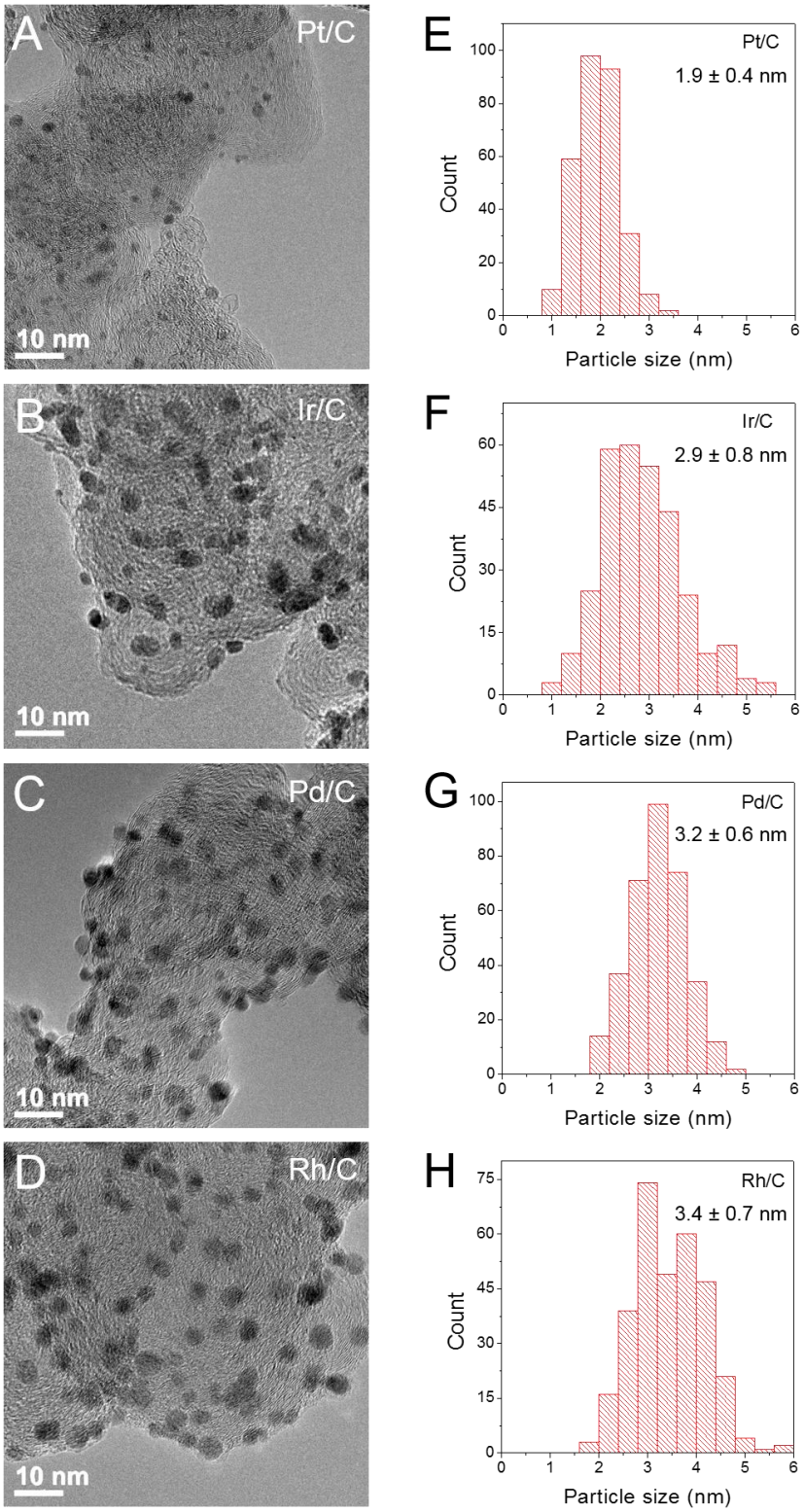

Fig. S14. TEM images and histograms of Pt, Ir, Pd, and Rh/C. TEM images of (**A**) Pt/C, (**B**) Ir/C, (**C**) Pd/C and (**D**) Rh/C and their corresponding histograms of particle size (**E-H**), the particle size is 1.9 ± 0.4 nm for Pt/C, 2.9 ± 0.8 nm for Ir/C, 3.2 ± 0.6 nm for Pd/C and 3.4 ± 0.7 nm for Rh/C.

The number averaged particle size (d_n) was calculated as follows

$$d_n = \frac{\sum_{i=1}^{n} d_i}{n} \qquad \text{(S9.1)}$$

where d_i is the individual particle diameter, and n is the number of particles measured.

The volume/area averaged particle size ($d_{v/a}$) is more accurate to represent the specific surface area than the number averaged particle size, which can be calculated as follows

$$d_{v/a} = \frac{\sum_{i=1}^{n} d_i^3}{\sum_{i=1}^{n} d_i^2} \qquad \text{(S9.2)}$$

The surface area determined from $d_{v/a}^{TEM}$ ($S_{v/a}^{TEM}$) was calculated by

$$S_{v/a}^{TEM} = \frac{6}{\rho d} \times 10^3 \qquad \text{(S9.3)}$$

where ρ is the density of the metal (21.45 g/cm^3 for Pt, 22.56 g/cm^3 for Ir, 12.02 g/cm^3 for Pd, and 12.41 g/cm^3 for Rh), d is the particle size in nm, $S_{v/a}^{TEM}$ is in unit of m^2/g.

10. Procedure for calculating pH for buffer solutions and comparison between calculated and experimental values

The buffer solutions were prepared by adding x ml ($0 < x < 14$) 4 M KOH into 100 ml 0.2 M H_3PO_4, 100 ml 0.2 M $KHCO_3$, 100 ml 0.2 M citric acid, 0.2 M acetic acid and 0.2 M boric acid to obtain phosphate buffer solutions, carbonate/bicarbonate buffer solutions, citrate buffer solutions, acetate buffer solutions and borate buffer solutions, respectively.

Their final pH (or $[H^+]$) can be calculated as follows using phosphoric acid as an example:

Phosphoric acid (H_3PO_4)

$H_3PO_4 \leftrightarrow H^+ + H_2PO_4^-$ $\quad pK_a1 = 2.15$

$H_2PO_4^- \leftrightarrow H^+ + HPO_4^{2-}$ $\quad pK_a2 = 7.20$

$HPO_4^{2-} \leftrightarrow H^+ + PO_4^{3-}$ $\quad pK_a3 = 10.35$

Mass balance:

$$[H_3PO_4]_0 = [H_3PO_4] + [H_2PO_4^-] + [HPO_4^{2-}] + [PO_4^{3-}] \quad \text{(S10.1)}$$

Charge balance:

$$[K^+] + [H^+] = [OH^-] + [H_2PO_4^-] + 2[HPO_4^{2-}] + 3[PO_4^{3-}] \quad \text{(S10.2)}$$

$$K_a1 = \frac{[H^+][H_2PO_4^-]}{[H_3PO_4]} \quad \text{(S10.3)}$$

$$K_a2 = \frac{[H^+][HPO_4^{2-}]}{[H_2PO_4^-]} \quad \text{(S10.4)}$$

$$K_a3 = \frac{[H^+][PO_4^{3-}]}{[HPO_4^{2-}]} \quad \text{(S10.5)}$$

$$K_w = [H^+][OH^-] \quad \text{(S10.6)}$$

We know $[H_3PO_4]_0$ and $[K^+]$, the six unknowns $[H_3PO_4]$, $[H_2PO_4^-]$, $[HPO_4^{2-}]$, $[PO_4^{3-}]$, $[H^+]$ and $[OH^-]$ can be obtained by solving Eqs S10.1-S10.6.

The pK_a values for $KHCO_3$, citric acid, acetic acid and boric acid are as follows:

Potassium bicarbonate ($KHCO_3$)

$H_2CO_3 \leftrightarrow H^+ + HCO_3^-$ $\quad pK_a1 = 6.30$

$HCO_3^- \leftrightarrow H^+ + CO_3^{2-}$ $\quad pK_a2 = 10.33$

Citric acid

$pK_a1 = 3.13$, $pK_a2 = 4.76$, $pK_a3 = 6.40$

Acetic acid (CH_3COOH)

$pK_a = 4.80$

Boric acid (H_3BO_3)

$B(OH)_3 \leftrightarrow BO(OH)_2^- + H^+$ $pK_a1 = 9.24$

$BO(OH)_2^- \leftrightarrow BO_2(OH)_2^{2-} + H^+$ $pK_a2 = 12.40$

$BO_2(OH)_2^{2-} \leftrightarrow BO_3^{3-} + H^+$ $pK_a3 = 13.30$

The pH values of the other four buffer solutions were calculated in the same matter as in the case of phosphate buffer solutions.

Experimentally measured pH values of the electrolytes from HOR/HER equilibrium potentials for HOR/HER polarization curves according to Eq. S11 in the manuscript match well with those theoretically calculated by method mentioned above (Fig. S15), indicating the reliability of pH determination using electrochemical method.

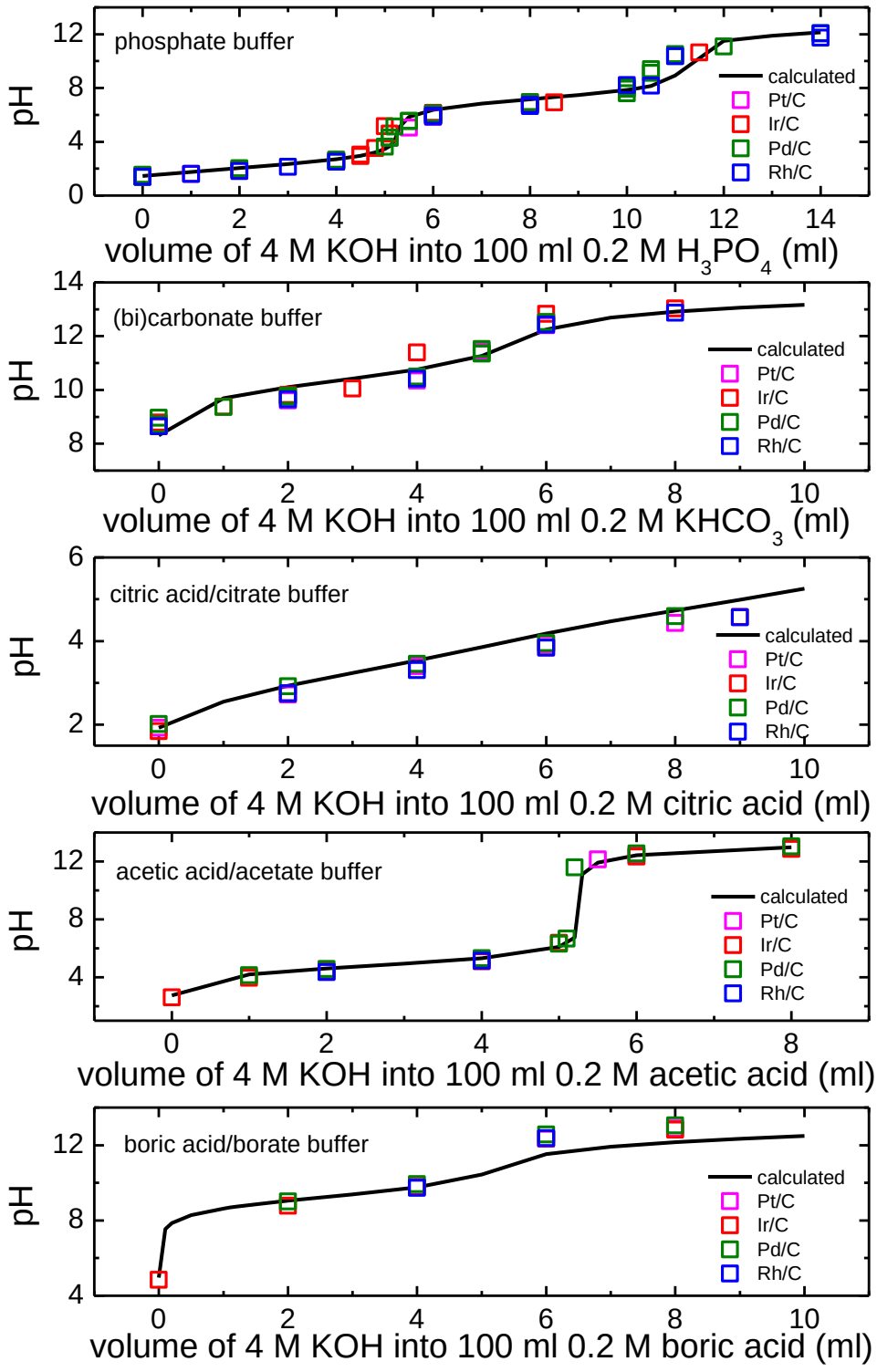

Fig. S15. **Comparison of calculated and electrochemically measured pH of the electrolytes.** Calculated (black line) and experimental measured pHs (hollow square) as a function of the volume of 4M KOH (mL) added into 100 ml 0.2 M H_3PO_4, $KHCO_3$, citric acid, acetic acid and boric acid.

11. HOR/HER polarization curves on Vulcan XC-72 in electrolytes with different pH values

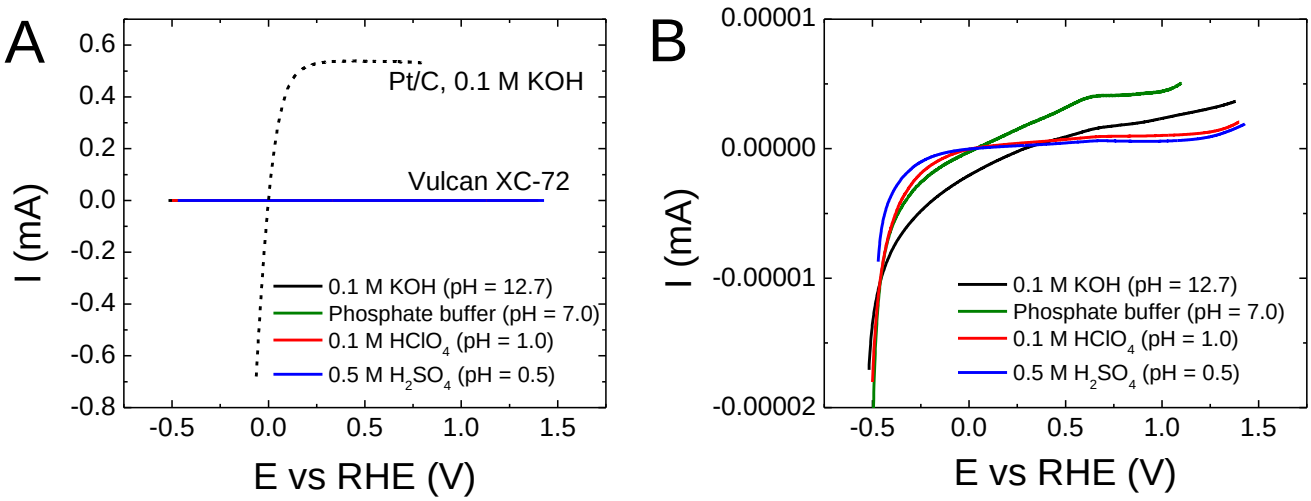

Fig. S16. **HOR/HER polarization curves on Vulcan XC-72.** (A) Polarization curves on Vulcan XC-72 in 0.1 M KOH (pH = 12.7) (solid black line), phosphoric acid/phosphate buffer (pH = 7.0) (solid green line), 0.1 M $HClO_4$ (pH = 1.0) (solid red line) and 0.5 M H_2SO_4 (pH = 0.5) (solid blue line) measured in H_2 at a scanning rate of 10 mV/s and a rotating speed of 1600 rpm. The loading of carbon on the glassy carbon electrode is 0.1 mg/cm2disk. The dash black line represents HOR/HER polarization curve on Pt/C in H_2-saturated 0.1 M KOH at a scanning rate of 1 mV/s and a rotating speed of 1600 rpm for comparison. The loading of Pt is 8 μg/cm^2_{disk}. (B) Zoom in polarization curves on Vulcan XC-72 in (A).

The HOR/HER on carbon supported Pt, Ir, Pd and Rh are contributed by the precious metals since carbon alone show negligible HOR/HER activity in electrolytes with pH range from about 0 to 13 (Fig. S16).

Table S1. Particle size and surface area of Pt/C, Ir/C, Pd/C, and Rh/C. Number averaged (d_n^{TEM}) and volume/area averaged ($d_{v/a}^{TEM}$) particle size from TEM, surface area calculated from $d_{v/a}^{TEM}$ ($S_{v/a}^{TEM}$) and electrochemical surface area determined from CV in 0.1 M KOH ($ECSA_{CV}$) and CO stripping in 0.1 M KOH ($ECSA_{CO\text{-}stripping}$) of Pt/C, Ir/C, Pd/C and Rh/C

	d_n^{TEM} (nm)	$d_{v/a}^{TEM}$ (nm)	$S_{v/a}^{TEM}$ (m^2/g)	$ECSA_{CV}$ (m^2/g)	$ECSA_{CO\text{-}stripping}$ (m^2/g)
Pt/C	1.9 ± 0.4	2.12	132	64 ± 9	103 ± 6
Ir/C	2.9 ± 0.8	3.34	80	64 ± 9	71
Pd/C	3.2 ± 0.6	3.38	148	78 ± 8	96
Rh/C	3.4 ± 0.7	3.73	130	80 ± 12	143 ± 18

Table S2. Effect of anions on H_{upd} peak potentials and HOR/HER exchange current densities. Surface area measured from H_{upd} adsorption and desorption peaks, potentials for Pt(110) and Pt(100) and the corresponding exchange current densities (i_0) in 0.1 M KOH with addition of various salts

Electrolyte	Surface area (cm^2)	Peak(110)(V)	Peak(100)(V)	i_0 (mA/cm^2_{Pt})
0.1 M KOH	0.303	0.276	0.393	0.805
0.1 M KOH + 0.1 M KCl	0.280	0.276	0.392	0.679
0.1 M KOH + 1 M KCl	0.244	0.266	0.377	0.590
0.1 M KOH + 0.1 M K_2SO_4	0.293	0.265	0.381	0.763
0.1 M KOH + saturated (~0.64 M)K_2SO_4	0.230	0.261	0.359	0.483
0.1 M KOH + 0.1 M $NaClO_4$	0.310	0.271	0.391	0.893
0.1 M KOH + (<) 1 M $NaClO_4$	0.244	0.271	0.385	0.428